Diagnosis of glioma by multivoxel ^{1}H-MRSI *

QUAN Hong[1], LIU Yue[2], BAO Shanglian[1]**, LI Shaowu[2], XIE Yaoqin[1], MIAO Binghe[1] and WANG Huiliang[1]

(1. Research Center for Tumor Diagnosis and Radiotherapeutical Physics and Laboratory of Medical Physics & Engineering, Peking University, Beijing 100871, China; 2. Neuro-Imaging Center, Beijing Neurosurgical Institute, Beijing 100050, China)

Received December 16, 2003; revised February 18, 2004

Abstract Glioma is one of the most malignant tumors due to its special construction of the glia cells and its character of infiltration. The usual procedure of the treatment is the surgical resection followed by radiotherapy with or without chemotherapy. This combined treatment needs the precise information on the extent of the tumor's infiltration and tumor grading, and then the determination can be made as to when, where and what kind of treatment should be used. Functional imaging modalities display advantages in defining the heterogeneous characters and histological grade. This paper describes how the ratios of Cho/NAA and Lac/NAA measured by magnetic resonance spectroscopy imaging (MRSI) could be used to define the cancer cell distribution in tissues, tumor burden and malignancy, and the results are proved to be consistent with the histological observation.

Keywords: segmentation of glioma, data analysis of MRSI, functional imaging for tumor diagnosis and treatment.

Glioma accounts for the majority of primary brain cancers in adults with a very poor prognosis[1~4]. The usual procedure of the treatment in clinical is the surgical resection followed by radiotherapy with or without chemotherapy. At present, using different treatments to control tumor's growth and avoid injury of sensitive brain tissues is the goal to achieve. But the key is how to segment the exact zone for these treatments, and this is precisely based on the definition of tumor infiltration and histological grading. Although magnetic resonance imaging (MRI) can provide a high resolution of morphological structure and has the capabilities to assess blood-brain-barrier (BBB) permeability with contrast media administration, it is limited by the failure of detecting earlier lesions and determining precise tumor margins, especially in the case that the tumor cells already infiltrated into normal parenchyma[5~7]. Functional imaging modalities display advantages in defining the heterogeneous characters and histological grade. Proton magnetic resonance spectroscopy imaging (^{1}H MRSI) has been shown to be an effective tool for noninvasive studies in patients with glioma[8~17]. ^{1}H MRSI could supply information on metabolites distribution, which may distinguish the normal and abnormal tissues for glioma patients. Up to now, there are several quantitive or semiquantitive methods of ^{1}H MRSI developed to analyze and evaluate tumor malignancy, and the methodology has evolved from single voxel to multivoxel, and from single to multislice ^{1}H MRSI[9~11, 16].

Despite these efforts, ^{1}H-MRSI has not yet become a routine method for diagnosis of gliomas. This is partly due to the lack of definite interpretation of ^{1}H-MRSI data in heterogeneous lesions or lesions that have received radiation therapy. Another barrier to its use is that, at present, there is no standardized method for determining what is normal for a given patient. Mcknight et al. proposed a residual z-score method to distinguish normal tissue from tumor infiltration and to evaluate the histological grade of glioma. However, this method needs to be corrected in the case of the tumor with a relatively large mass, and it is not suitable for mapping lactate/lipid (Lac), which is an important marker indicating the malignancy of glioma.

To solve this problem, we use two different statistical models to form a map, in which the tumor margin, high activity region and malignancy of tumor are clearly demonstrated. The results are verified by the histological observations.

* Supported by the National Natural Science Foundation of China (Grant Nos. 10275003 and 10175004) and the Natural Science Foundation of Beijing (Grant No. 3011002)

** To whom correspondence should be addressed. E-mail: bao@pku.edu.cn

1 Materials and methods

1.1 Magnetic resonance spectroscopy imaging

All MR data were acquired with a 3T GE Signa scanner equipped with a quadrature head coil. Each examination began with a series of MR imaging sequences, which always included a pre- or postgadolinium enhanced inversion recovery (IR) echo with the parameters of TR/TE/TI=2400/24/860, flip=90°, 256×256 matrix, 240 mm FOV, 1 NEX, 5 mm slices. The IR volume was used as a reference for the multivoxel MRSI study. After IR imaging, the two-dimensional chemical shift imaging (2D-CSI) with the point resolved spectroscopy (PRESS) was used to measure the spectra of choline (Cho), creatine (Cr), N-acetylaspartate (NAA), and lactate/lipid (Lac) in the region containing both the lesion and normal-appearing tissue. The parameters in 2D-CSI were TR/TE=2000/144, PHASE encode matrix=256×16. Water suppression was achieved with additional chemical shift selective (CHESS) pulses.

After each examination, both the images and raw spectral data were transferred to a Sun Ultra 10 Workstation for processing. An automatic search procedure was used to identify each resonance peak of the metabolites. The spectra were quantified by both peak height (PH) and integrated peak area (IPA). The peak positions of Cho, Cr, NAA, and Lac were located at 3.2 ppm, 3.0 ppm, 2.0 ppm, and 1.3/1.7 ppm respectively. The parameters of the spectra were then overlapped with the enhanced IR image.

1.2 Statistical model

Mcknight et al. developed an automatic statistical analysis method for identifying a control population of spectra acquired from normal tissue from the contralateral hemisphere of the studied patients[16]. The model was based on two assumptions. The first assumption was that the variation in cell density due to partial volume effects did not significantly affect the relative ratio of Cho to NAA in normal brain tissue. The second assumption was that the variation of the Cho to NAA (or Cr) ratio in normal brain was small when compared with the difference between normal and diseased brain. With these assumptions in mind, the Cho level could be plotted against the NAA and fit with a linear regression. Then the residual-μ (μ: mean value) and standard deviation (SD) of the perpendicular residual distance between each point and the regression line were estimated. The criterion for normality was a z-score [(residual-μ)/SD] of less than 2, which corresponds to 95% probability of that the voxel belonged to the fitted population. Points that did not meet the criterion were excluded from the model, and a new regression line was calculated through the remaining points. This process was repeated until no points were excluded. The remaining points were the control population that was used to estimate the normal ratios of Cho/NAA and Cho/Cr. Once the control population of points was defined, the residual z-score of each voxel within the PRESS box was calculated and was used as an estimation of the probability for the presence of disease.

The z-score model was well fitted to the relative small size of glioma, but it was difficult to analyze the data from large mass tumors. In the case of large size of glioma, the number of abnormal voxels was usually larger than the normal ones within the PRESS box. Thus, a new threshold was suggested for calculating the Cho/NAA (or Cho/Cr) ratio of the normal tissue within the PRESS region, only those voxels whose Cho/NAA (or Cho/Cr) ratio value was below the thresholds were considered, in which threshold=1 for Cho/NAA and threshold=1.5 for Cho/Cr in this study.

Lac, which is produced in tumor cells by glycolysis, is not only the product of anaerobic glucose metabolism caused by inadequate oxygen supply, but also a possible aerobic process that may lead to formation of this compound. Lac is usually presented in high-grade glioma and absent in most low-grade glioma, and NAA is usually reduced greatly in all grades of glioma[9, 13~16]. Thus, the value of Lac/NAA may be effective in determining the tumor malignancy. Because Lac concentration could not be detected from the normal brain and even from most low grade glioma, the residual z-score model is not fitted to the Lac/NAA ratio. Thus, The Lac/NAA value rather than the residual z-score model was used to assess the histological grade of glioma.

In order to define the tumor margin, tumor burden or high activity region, and histological grade for each patient, two different statistic models could be used to form a map. Among them, tumor margin corresponded with z-scores above the value of 2, tumor burden or high activity region was consistent with the mean z-scores from the excluded voxels, and the Lac/NAA value above 0.6 indicated the presence

of Lac which might be associated with hypoxia and malignancy.

1.3 Human subjects

The human subjects involved in our study were 9 patients with glioma including 4 female and 5 male subjects, aged from 33 to 56 years old. Patients were first diagnosed by MRI and MRSI examinations, then treated by surgery. The biopsy samples were taken during the surgery and sent to the laboratory for pathological observation. The diagnosis was made for the 9 patients: 4 cases were at grade Ⅳ, 2 cases at grade Ⅲ, and 3 cases at grade Ⅱ.

2 Results

Plate IA illustrates the results of a primary glioma of grade Ⅳ. The T_1-weighted image showing the enhanced lesion with an overlaid image of the PRESS box is displayed in (a), and the corresponding spectra are shown in (b). The contour defined by red line represents the tumor margin, the contour defined by yellow line represents the tumor burden or metabolic activity, the contour defined by fuchsine line represents the most abnormal voxels of z-score; and the black line represents the appearance of the Lac, the bluish line represents the relative high value of the Lac concentration corresponding to the mean of the Lac/NAA ratio above 0.6. In Plate IA, (c) and (d) show the results of PH, while (e) and (f) show the results of IPA. The images of the z-score reflect the heterogeneity of the lesion seen in MRI.

Plate IB demonstrates the compared results of different z-scores, Cho/NAA and Cho/Cr, to define tumor margin and high metabolic activity from a grade Ⅳ patient. The results of the PH are presented in (a), while the results of the IPA are shown in (b). Apparently, the two different residual z-scores correspond to each other. In Mcknight et al.'s study, the PH qualification was more credible than the IPA[16]. We may draw the same conclusion from our study. The Cho/NAA of the control voxels calculated by PH of the 9 patients is 0.66 ± 0.05, and Cho/NAA of the control voxels calculated by IPA is 0.61 ± 0.11 which is double the standard deviation. Therefore, PH is used to quantify the relative metabolite levels in our study, because the value of PH is less influenced by random noise.

The results from the glioma patients analyzed by our method are summarized in Table 1. Our results are consistent with Mcknight et al.'s study and support the idea that the z-scores increase with the onset of malignancy and decrease in glioma with necrosis[16]. There is no Lac detected in grade Ⅱ glioma. The mean values of the Lac/NAA above 0.6 in grade Ⅲ and Ⅳ patients are 1.13 and 2.64, and the maximum value of the Lac/NAA in grade Ⅲ and Ⅳ patients is 1.36 and 7.37, respectively. Apparently, the ratio of the Lac/NAA is positively correlated to the malignancy of glioma. Plate IC demonstrates the results from three glioma patients. It can be seen that the region of the relatively high Lac concentration, which is possibly related to hypoxia or necrosis, is located outside the most malignant region of glioma, indicating that Cho is greatly reduced in the necrotic tissue.

Table 1. Residual z-scores and metabolite ratios in patients with glioma

	Cho/NAA z-scores[a)]		Cho/Cr z-scores[b)]		Lac/NAA (≥0.6)	
	Average z-scores	Maximum z-scores	Average z-scores	Maximum z-scores	Average	Maximum
Grade Ⅱ	5.16 ± 1.08	8.44 (5.67~10.85)	5.88 ± 1.17	10.41 (7.76~13.31)	—	—
Grade Ⅲ	11.58 ± 3.47	24.12 (21.22~27.02)	10.10 ± 3.33	24.07 (19.52~28.61)	1.13	1.36
Grade Ⅳ	7.30 ± 1.83	15.81 (9.95~25.97)	9.53 ± 2.67	21.33 (8.19~33.66)	2.64	7.37

a) The ratio of Cho/NAA of the control voxel is 0.66 ± 0.05; b) the ratio of Cho/Cr of the control voxel is 1.05 ± 0.10.

3 Discussion and conclusion

Because the Lac concentration could not be detected from the normal brain and even from most of low grade glioma[13~16], we used two different models for evaluating tumor margin, tumor burden or metabolic activity (z-score), and the malignancy (the ratio of Lac/NAA), and the measured values were consistent with the pathological observations. We also tried to depict the region of hypoxia in glioma for it is closely related to the efficiency of radiotherapy. However, it could not be achieved only using our method so it still needs to be confirmed by pathological diagnosis.

Although it appears that MRSI holds great promise as an aid in diagnosis and treatment of the brain tumor, it still has problems and limitations. One of the problems in use of MRSI is related to the size and shape of the excited region (defined by

PRESS box)[9, 16]. This will lead to the consequence that the PRESS box could not cover the entire tumor volume without subcutaneous lipid. Especially in the case of large size of tumor, some threshold values have to be installed to ensure the z-score method running smoothly. This modification of the z-score model needs to be verified in our further clinical tests. Another limitation of the MRSI is the spatial resolution. The nominal voxel of MRSI in 3T GE Signa scanner is $7.5\times 7.5\times 15\ mm^3$ (in our test it was $7.5\times 7.5\times 20\ mm^3$). It is difficult to explain what the z-score for a given voxel means in terms of metabolic activity. Thus, the spatial resolution of MRSI and the sensitivity of RF coil need to be further improved[9].

References

1 Chang, C. H. et al. Comparison of postoperative radiotherapy and combined postoperative radiotherapy and chemotherapy in the multidisciplinary management of malignant gliomas. A joint radiation therapy oncology group and eastern cooperative oncology group study. Cancer, 1983, 53: 999.

2 Davis, L. W. Malignant glioma—A nemesis which requires clinical and basic investigation in radiation oncology. Int. J. Radiat. Oncol. Biol. Phys., 1989, 16: 1355.

3 Shapiro, W. R. Therapy of adult malignant brain tumors: What have the clinical trials taught us? Semin. Oncol., 1986, 13: 38.

4 Fine, H. A. et al. Meta-analysis of radiation therapy with and without adjuvant chemotherapy for malignant gliomas in adults. Cancer, 1993, 71: 2585.

5 Brunetti, A. et al. Functional characterization of brain tumors: an overview of the potential clinical value. Nuclear Medicine & Biology, 1996, 23: 699.

6 Leibel, S. A. et al. Loeffler contemporary approaches to the treatment of malignant gliomas with RT. Seminars in Oncology, 1994, 21(2): 198.

7 Watanabe, M. et al. Magnetic resonance imaging and histopathology of cerebral gliomas. Neuroradiology, 1992, 34: 463.

8 Isobe, T. et al. Quantification of cerebral metabolites in glioma patients with proton MR spectroscopy using T2 relaxation time correction. Magnetic Resonance Imaging, 2002, 20: 343.

9 Pirzkall, A. et al. MR-spectroscopy guided target delineation for high-grade glioma. Int. J. Radiat. Oncol. Biol. Phys., 2001, 50(4): 915.

10 Tamawski, R. et al. ^{1}H-MRS *in vivo* predicts the early treatment outcome of postoperative radiotherapy for malignant gliomas. Int. J. Radiat. Oncol. Biol. Phys., 2002, 52(5): 1271.

11 Walecki, J. et al. Role of short TE 1H-MR spectroscopy in monitoring of post-operation irradiated patients. European Journal of Radiology, 1999, 30: 154.

12 Hamilton, R. J. et al. Functional imaging in treatment planning of brain lesions. Int. J. Radiat. Oncol. Biol. Phys., 1997, 37(1): 181.

13 Luyten, P. R. et al. H^1 MR spectroscopic imaging and PET. Radiology, 1990, 176: 791.

14 Fulham, M. J. et al. Mapping of brain tumor metabolites with proton MR spectroscopic imaging: clinical relevance. Radiology, 1992, 185: 675.

15 Duyn, J. H. et al. Multisection proton MR spectroscopic imaging of the brain. Radiology, 1993, 188: 277.

16 Mcknight, T. R. et al. An automated technique for the quantitative assessment of 3D-MRSI data from patients with glioma. JMRI, 2001, 13: 167.

17 Shukla-Dave, A. et al. Prospective evaluation of *in vivo* proton MR spectroscopy in differentiation of similar appearing intracranial cystic lesions. MRI, 2001, 19: 103.

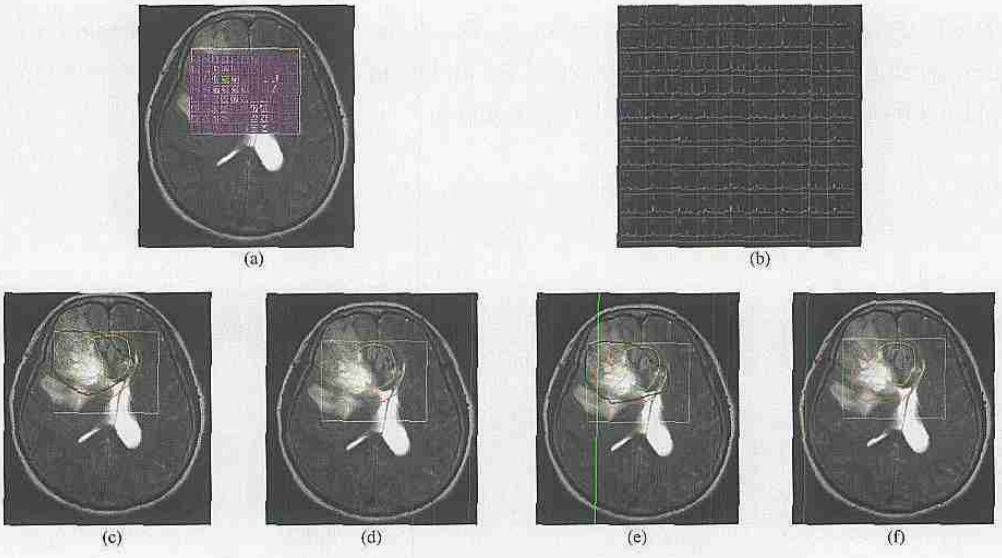

(a) (b) (c) (d) (e) (f)

A. A primary glioma of grade Ⅳ, (a) Contrast-enhancement T1w MRI overlaid the PREEE-box; (b) The corresponding *MRS*; (c) Cho/NAA z-scores and Lac/NAA; (d) Cho/Cr z-scores; (e) Cho/NAA z-scores and Lac/NAA; (f) Cho/Cr z-scores. (c) and (d) Quantification by *peak height*, (e) and (f) Quantification by integrated peak area.

(a) (b)

B. Comparson of different z-scores, Cho/NAA (red line) and Cho/Cr (green line), to define tumor margin (real line), high metabolic activity (dotted line) and the most abnormal voxels (the fuchsine real line) from a patient of grade Ⅳ. *(a) Calculated by peak height, (b) calculated* by integrated peak area.

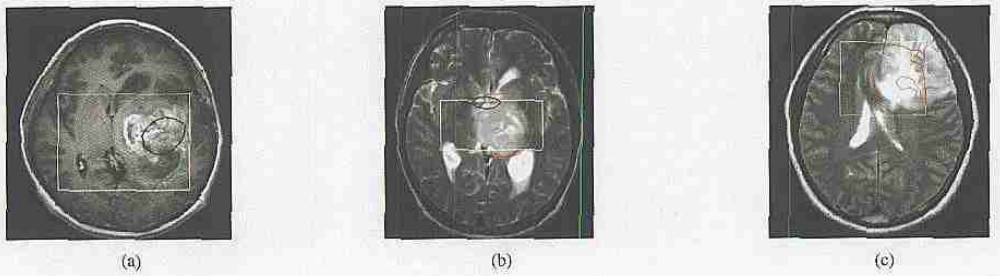

(a) (b) (c)

C. Correlation between Lac/NAA and malignancy of glioma. The red line contours tumor margin, the fuchsine line contours the most abnormal voxels; the black line contours the appearance of Lac, and the bluish line corresponds to the region of probable anoxia. Noted that there is no Lac detected in grade Ⅱ glioma. (a) From a grade Ⅳ patient, (b) from a grade Ⅲ patient, (c) from a grade Ⅱ patient.